PROF. XM YIN (Orcid ID : 0000-0002-8576-6093)

Article type : Original

Hepatic Autophagy Deficiency Compromises FXR Functionality and Causes Cholestatic Injury

Bilon Khambu[1], Tiangang Li[2], Shengmin Yan[1], Changshun Yu[1, 3], Xiaoyun Chen[1], Michael Goheen[1], Yong Li[1], Jingmei Lin[1], Oscar W. Cummings[1], Youngmin A. Lee[4, 5], Scott Friedman[4], Zheng Dong[6, 7], Gen-Sheng Feng[8], Shangwei Wu[9], Xiao-Ming Yin[1, 3 *]

[1]Department of Pathology and Laboratory Medicine, Indiana University School of Medicine, Indianapolis, IN, USA; [2]Department of Pharmacology, Toxicology and Therapeutics, The University of Kansas Medical Center, Kansas City, KS, USA; [3]Kingmed School of Laboratory Medicine, Guangzhou Medical University, Guangzhou, Guangdong, China; [4]Department of Medicine, Mount Sinai Medical School, New York, NY, USA; [5]Laboratory of RNA Molecular Biology, The Rockefeller University, New York, NY, USA; [6]Department of Nephrology, The Second Xiangya Hospital, Central South University, Changsha, Hunan, China; [7]Department of Cell Biology and Anatomy, Medical College of Georgia at Augusta University and Charlie Norwood VA Medical Center, Augusta, GA, USA; [8]Department of Pathology, University of California at San Diego, San Diego, CA, USA; [9]Center of Pathology and Laboratory Medicine, Nankai Hospital, Tianjin, China

Keywords:

Atg7, Bile acids, BSEP, Cholestasis, NRF2

* Corresponding Author. Xiao-Ming Yin

Department of Pathology and Laboratory Medicine, Indiana University School of Medicine, Indianapolis, IN 46202
Phone: 317-274-1779, Fax: 317-491-6639, Email: xmyin@iupui.edu

Financial Support: The authors are in part supported by NIH grants R01AA021751 (XMY), R21AA021450 (XMY), and R01DK10248 (T.L.). YAL was supported in part by grant #UL1TR001866 from the National Center for Advancing Translational Sciences, the CSTA program of NIH and the German Research Foundation (LE 2794/1-1). The funding source does not participate in the study design or execution.

This is the author's manuscript of the article published in final edited form as:

Khambu, B., Li, T., Yan, S., Yu, C., Chen, X., Goheen, M., … Yin, X.-M. (2019). Hepatic Autophagy Deficiency Compromises FXR Functionality and Causes Cholestatic Injury. Hepatology, 0(ja). https://doi.org/10.1002/hep.30407

Accepted Article

Accepted Article

Conflict of Interest
Dr. Dong consults for Renasym

Abbreviations:
ABCG5, ATP Binding Cassette Subfamily G Member 5; ABCG8, ATP Binding Cassette Subfamily G Member 8; AKR1D1, 3-oxo-5-beta-steroid 4-dehydrogenase; APOE, Apolipoprotein E; ARE, Antioxidant Response Element ; ATG5, Autophagy-related gene 5; ATG7, Autophagy-related gene 7; BA, Bile Acids; BAAT, Bile acid-CoA:amino acid N-acyltransferase; BACS, Bile acyl-CoA synthetase; BSEP, Bile salt export pump; CA, Cholic acid; CDCA: Chenodoxycholic acid; CYP27A1, Sterol 26-hydroxylase, mitochondrial; CYP7A1, Cholesterol 7-alpha-monooxygenase; CYP7B1, 25-hydroxycholesterol 7-alpha-hydroxylase; CYP8B1, 7-alpha-hydroxycholest-4-en-3-one 12-alpha-hydroxylase; CYP27A1: Sterol 26-hydroxylase, mitochondrial; FXR, Farnesoid X receptor; HMGB1, High mobility group box 1; HMGB1: High mobility group box 1; HSD3B7, 3 beta-hydroxysteroid dehydrogenase type 7; KEAP1, Kelch-like ECH-associated protein 1; LC3B, Light Chain3 beta; MDR1A, Multidrug resistance protein 1a; MDR1B, Multidrug resistance protein 1b; MDR2, Multidrug resistance protein 2; MRP2, Multidrug resistance-associated protein 2; MRP3, Multidrug resistance-associated protein 3; MRP4, Multidrug resistance-associated protein 4; mTOR, Mammalian target of rapamycin; NRF2, Nuclear factor erythroid 2-related factor 2; NTCP, Na^+-taurocholate cotransporting polypeptide; OATP, organic-anion-transporting polypeptide; OSTβ, Organic solute transporter beta; PEPCK, Phosphoenolpyruvate carboxykinase; SHP, Small Heterodimer Partner; SLC27A1, Solute Carrier Family 27 Member 5; TCA, Taurocholic acid; TMCA, Tauromuricholic acid; ZO-1, Zonula occludens-1.

ABSTRACT

Autophagy is important for hepatic homeostasis, nutrient regeneration and organelle quality control. We investigated the mechanisms by which liver injury occurred in the absence of autophagy function. We found that mice deficient in autophagy due to the lack of *Atg7* or *Atg5*, key autophagy-related genes, manifested intracellular cholestasis with increased levels of serum bile acids, a higher ratio of TMCA/TCA in the bile, increased hepatic bile acid load, abnormal bile canaliculi and altered expression of hepatic transporters. In determining the underlying mechanism, we found that autophagy sustained and promoted the basal and upregulated expression of *Fxr* in the fed and starved conditions, respectively. Consequently, expression of *Fxr* and its downstream genes, particularly *Bsep*, and the binding of FXR to the promoter regions of these genes, were suppressed in autophagy-deficient livers. In addition,

This article is protected by copyright. All rights reserved.

co-deletion of *Nrf2* in autophagy deficiency status reversed the FXR suppression. Furthermore, the cholestatic injury of autophagy-deficient livers was reversed by enhancement of FXR activity or expression, or by *Nrf2* deletion. ***Conclusions*:** Together with earlier reports that FXR can suppress autophagy our new findings indicate that autophagy and FXR form a novel regulatory loop and deficiency of autophagy causes abnormal FXR functionality, leading to the development of intracellular cholestasis and liver injury.

INTRODUCTION

Macroautophagy, hereafter referred to as autophagy, is an evolutionarily conserved cellular degradation mechanism dependent on the lysosome (1). It is important for nutrient regeneration, organelle turnover, clearance of aggregated cellular materials, and defense against intracellular pathogens. Autophagy is well regulated for the need for nutrients and energy, and the catabolic function of autophagy is often coupled with the anabolic need of the cell (2-4). However, the regulation of metabolism by autophagy via mechanisms other than recycling macromolecules or organelles is not well studied.

Autophagy deficiency can result in multiple pathological conditions (5). Deficiency in hepatic autophagy causes severe hepatomegaly and liver injury, accompanied with inflammation fibrosis and tumorigenesis (6-8). How loss of autophagy function leads to the pathological consequences in the liver and other tissues is not well understood but is likely caused by more than just failure in degradation of pathogenic constituents. In the liver it is found that the accumulation of p62/SQSTM1 disabled the ubiquitination process of NRF2 (6). As the result, NRF2 is accumulated and contributes to the liver injury phenotype (6-8).

However, it is not known how NRF2 mediates hepatic injury. We have found that NRF2 can control the release of HMGB1 from hepatocytes (8). HMGB1 affects some of the phenotypic presentations of the autophagy-deficient liver, including ductular reaction and

This article is protected by copyright. All rights reserved.

Accepted Article

tumor development, but not the injury. Thus there would be other NRF2-directed events that contribute to the development of liver injury. NRF2 is known as a transcription activator, binding to the promoter region of many target genes at the sequence site known as antioxidant response element (ARE) (9-11). NRF2 is often activated in response to oxidative stress or electrophilic stress (11, 12), and many of the target genes are involved in anti-oxidative response. In addition, it transcriptionally activates a number of enzymes for oxidation/reduction, conjugation and transportation of drugs (11, 13). These activities are generally associated with a cellular protective role of NRF2. However, alterations in gene functions caused by NRF2 that may result in tissue injury have not been defined.

The present study found that autophagy deficiency can lead to multiple defects related to bile acids (BA) synthesis, secretion and regulation, and autophagy deficient mice presented a phenotype consistent with intracellular cholestasis, which can contribute to the liver injury in these mice. Notably NRF2 is instrumental in the development of these phenotypes. Moreover, FXR stands out as an important target regulated by autophagy function in both fed and starved conditions. Recovery of FXR functionality in autophagy deficient livers is able to remedy the disturbed BA metabolism and the cholestasis phenotype. Since FXR can suppress the expression of some autophagy genes under nutrient replete condition (14, 15), the ability of autophagy to stimulate *Fxr* expression at basal and starvation condition indicate the two functions can form a regulatory loop, which is important for the homeostasis of the liver.

Materials and Methods

Mice and reagents. Mice with hepatic deletion of *Atg7* or *Atg5*, with or without *Nrf2* co-deletion, were bred as detailed in the Supplemental Methods. Mice of both genders at the age of 9-week old were studied. All animal procedures were approved by the institutional animal

This article is protected by copyright. All rights reserved.

Accepted Article

Accepted Article

care and use committee (IACUC) of the Indiana University. Antibodies used in this study are shown in **Supplemental Table S1**. Gene-specific primers (**Supplemental Table** S**2)** were ordered from Integrated DNA Technologies, Inc (Coralville, Iowa).

Biochemical, molecular, immunological and imaging assays. Blood chemistry and bile acids were analyzed using commercial available kits or by mass spectrometry. Histology and electron microscopy, immunoassys, qRT-PCR and CHIP analysis were performed using standard protocols. Additional details can be found in the Supporting Information.

Statistical analysis. Statistical analysis was performed using Sigma Stat 3.5 with information on distribution fitting and variance that were appropriate for the test selected. Results were expressed as the means ± s.e.m. *P* values from at least 3 independent determinations or samples per treatment were calculated using One-Way ANOVA followed by Duncan's post-hoc analysis (for multiple group comparisons) or two-tailed Student's t-test (for paired group comparisons). A *P* value of <0.05 was considered significant.

RESULTS

Autophagy deficiency caused NRF2-dependent cholestasis

Mice with autophagy deficiency in the liver developed hepatic injury (6, 7), but the nature of the injury and the involved mechanism were not known. Notably, the injury can be largely corrected by the co-deletion of *Nrf2* (6, 7). How could a normally anti-oxidative NRF2 become pathogenic in the autophagy-deficient condition is not understood. We found that mice deficient in hepatic *Atg7* (*Atg7*$^{\Delta Hep}$) had a significantly elevated level of serum bile acids (BA) but not total bilirubin (**Fig. 1A)**, and there was a lack of jaundice and obvious external bile duct blockage, all suggesting the presence of intracellular cholestasis. Concomitantly,

This article is protected by copyright. All rights reserved.

there was an elevated level of cholesterols but not triglycerides **(Fig. 1D**), consisting with an inhibition of synthetic conversion of cholesterol to BA during cholestasis. As reported before, live injury as measured by serum level of ALT (**Fig. 1C**) was significant. Together with the histological evidence of massive ductular reaction reported in our earlier studies (8), these findings suggest that the autophagy deficient livers had developed cholestatic injury.

Deletion of another key autophagy gene, *Atg5*, in the liver ($Atg5^{\Delta Hep}$) led to the same biochemical (**Fig. S1**) and histological (8) alterations. Remarkably, in both $Atg7^{\Delta Hep}$ and $Atg5^{\Delta Hep}$ mice, co-deletion of *Nrf2* corrected the abnormal levels of BA and cholesterol (**Fig. 1A-C, Fig. S1**), implicating that NRF2 contributed to the development of cholestasis.

Using a tamoxifen-inducible mouse strain of *Atg7* deletion ($Atg7^{Hep\text{-}ERT2}$), we found that elevation of blood BA was a rapidly developed early event that followed autophagy gene deletion in hepatocytes (**Fig. 1D**). Deletion of *Atg7* in the adult livers was apparent in 7 days after the administration of tamoxifen (see below). Elevations of blood BA, cholesterol and ALT were progressed in parallel, but BA elevation was earlier at Day 10 after tamoxifen treatment, followed by the elevations of cholesterol and ALT at Day 12, and Day 15, respectively.

While the BA levels in the gallbladder and the intestine were not changed, BA level in the liver was significantly increased (**Fig.1E**), indicating an accumulation in the hepatocyte. The total BA pool was only mildly increased in autophagy deficient mice (**Fig. 1F**), due to the larger size of the intestinal BA pool, which diminished the relative contribution of the hepatic BA to the total pool. However, when the total pool is normalized to the body weight, it was

This article is protected by copyright. All rights reserved.

Accepted Article

significantly higher in autophagy deficient mice (**Fig. 1F**), indicating an overall elevation of BA in the digestive track relative to the body size.

Bile acids metabolism was altered in autophagy deficient livers.

Bile acids are synthesized in hepatocytes via the classical and alternative pathways (**Fig. S2A**). All four key genes involved in BA synthesis, *Cyp7a1* and *Cyp8b1* of the classical pathway, and *Cyp27a1* and *Cyp7b1* of the alternative pathway, were reduced in expression in *Atg7*-deficient livers (**Fig. 2A. Fig. S2B)** or in *Atg5*-defient livers **(Fig. S2C**). Expression of *Hsd3b7*, but not *Akr1d1*, was also reduced in expression (**Fig. 2B-C**). These results could rule out that the elevated BA levels in the liver and in the blood were due to an increased expression of key synthesis enzymes. The results might be more compatible with the presence of feedback suppression during cholestasis. In addition, *Nrf2* co-deletion significantly reversed the change of these genes except *Cyp7b1* (**Fig. 2A-C, FigS2B**), indicating that *Nrf2* could be largely responsible for these expressional changes, although *Cyp7b1* seemed to be affected independently.

The composition of different BA species in the bile was thus analyzed (**Fig. 2D-E**). The majority of the mouse BA in the bile was conjugated with taurine, which did not seem to change in autophagy-deficient mice. There seemed to have a reduction in unconjugated primary BA and in conjugated or unconjugated secondary BA in autophagy deficiency. However, the most significant change was the increase in conjugated α- and β-muricholic acids (TMCA), and the corresponding decrease in conjugated cholic acids (TCA), leading to a higher TMCA/TCA ratio in the autophagy-deficient mice. In contrast, the control mice had a lower TMCA/TCA ratio as previously reported (16-19). This suggested an imbalance in the synthesis of different BA species in autophagy-deficient livers.

This article is protected by copyright. All rights reserved.

Accepted Article

This change in TMCA/TCA ratio is likely due to the mechanism that the synthesis of cholic acid (CA) but not chenodeoxycholic acid (CDCA) is dependent on CYP8B1 (**Fig. S2A**). In addition, the alternative pathway, which contributes mainly to CDCA, would be less affected by changes in mRNA expression of the relevant enzymes than by their post-transcriptional regulations (20). Together, these conditions led to a relatively higher level of CDCA, and thus a higher level of muricholic acids, which are derived from CDCA, similar to what has been reported in *Cyp8b1*-deficient mice (19).

***Nrf2* caused the absence of BSEP in autophagy deficient livers**

To explore the potential mechanism of cholestasis in the autophagy-deficient livers, we examined the expression of BA transporters. More than 95% of the synthesized BA are secreted into the bile canaliculi through bile salt export pump (BSEP/ABCB11), at the apical side of hepatocytes (21, 22), which is a major contributor of the bile acid-dependent bile flow. We found a greatly diminished protein expression of BSEP in both $Atg7^{\Delta Hep}$ and $Atg5^{\Delta Hep}$ livers (**Fig. 3A-B**). Immunostaining for BSEP demonstrated a distinct bile canaliculi pattern in normal, but not in autophagy-deficient, livers (**Fig. 3C**). Co-deletion of *Nrf2* restored the expression (**Fig. 3A-C**). Deficiency of BSEP could be at least in part responsible for the cholestasis (22, 23).

Three other apical transporters, *Mrp2/Abcc2*, *Mdr1a/Abcb1a*, and *Mdr1b/Abcb1b* were increased in mRNA expression (**Fig. 3D, Fig. S3A**), likely as a result of compensatory response to *Bsep* downregulation (22). These transporters account for only a low level of bile acid secretion, but were mainly involved in the secretion of bilirubin, GSH and organic ions (24). Two other apical transporters, *Mdr2/Abcb4*, mainly for the secretion of phospholipids (25), and *Abcg5* and *Abcg8*, which form heterodimer for the secretion of cholesterol (26), did not present significant changes in autophagy deficient livers (**Fig. 3D**).

This article is protected by copyright. All rights reserved.

Accepted Article

As seen in a variety of cholestatic conditions, the mRNA expression of basolateral-systemic transporters (*Mrp3, Mrp4,* and *Ostβ*) (**Fig. 3E, Fig. S3B-C**) was increased in both *Atg7*$^{\Delta Hep}$ and *Atg5*$^{\Delta Hep}$ livers for enhanced efflux of bile acids into the system circulation, which was consistent with the elevated BA in the blood (**Fig. 1A**). Concordantly, there was an anticipated reduction in the expression of the basolateral enterohepatic transporters (*Oatp, Ntcp*) (**Fig. 3F**) in order to reduce the reabsorption of BA from the enterohepatic circulation. Co-deletion of *Nrf2* also corrected the alterations in the expression of basolateral transporters (**Fig. 3E-F, Fig. S3B-C**), thus supporting the notion that *Nrf2* could mediate these changes under autophagy deficiency.

Autophagy deficiency caused abnormalities in bile canaliculi

The immunostaining pattern of MRP2, an apical transporter, seemed to be enhanced and was slightly distorted at certain locations (**Fig. 4A**). Electron microscopic analysis of the *Atg7*-deficient livers confirmed that bile canaliculi were swollen and dilated (**Fig. 4B**). Many of the canaliculi had fewer or no microvilli; and lamellar materials or proteinaceous deposits were observed inside the canaliculi. The alteration also involved the tight junction as shown by the staining for ZO-1 (**Fig. 4C**). Normal ZO-1 staining showed a mixed pattern of puncta and fine lines along the hepatocyte boards. However, in *Atg7*-deficient livers, a coarse, expanded, and twisted pattern was observed, which suggested a change in the bile canaliculi (27). Notably the ultrastructural alterations in bile canaliculi and the irregular MRP2 and ZO-1 immunostaining patterns were largely corrected when *Nrf2* was co-deleted (**Fig. 4A-C**).

While the cannalicular structure and the tight junctions were compromised, the adherens junction and the cytoskeletal components seemed to be largely preserved as shown by the normal β CATENIN expression pattern (**Fig. 4D**), and the normal F-actin staining pattern (**Fig. 4E**).

This article is protected by copyright. All rights reserved.

Accepted Article

Accepted Article

Autophagy regulates FXR expression in fed and starved conditions

Regulation of BA metabolism is complicated and is affected by multiple factors. We decided to focus on the potential role of FXR in the present case not only because FXR regulates BA metabolism at multiple points, including the transcriptional expression of *Bsep* and several other genes whose promoters contain FXR response elements (FXRE)(20, 28-32), but also because FXR had been shown to interplay with autophagy function in a negative fashion under the fed condition (14, 15). Autophagy function could in turn affect FXR; but this possibility had not been studied.

We thus examined whether FXR expression could be affected by the treatment of rapamycin or starvation. Either treatment blocks mTOR function and stimulates autophagy in a physiologically relevant manner from the yeast to the mammals (1). Indeed, we found that FXR expression was upregulated in wild type mice following such treatments (**Fig. 5A-B**). In addition, some FXR targets, such as *Pepck*, *ApoE*, and *Baat*, were significantly upregulated in both treatments, whereas other targets were only significantly upregulated in starved condition, such as *Shp* and *Slc27a5/Bacs*, or in neither condition, such as *Bsep*, in the same time frame (**Fig. 5B**).

We then compared the FXR expression in autophagy-competent and autophagy-deficient mice under the fed condition. In contrast to the condition of autophagy activation, hepatic expression of FXR was significantly reduced in both $Atg7^{\Delta Hep}$ and $Atg5^{\Delta Hep}$ mice (**Fig. 5C, Fig. S4A-B**). To rule out that this FXR reduction was a long-term adaptive response to autophagy deficiency we analyzed the time course of such changes in the inducible $Atg7^{\Delta Hep\text{-}ERT2}$ mice under the fed condition. FXR and BSEP expression decreased rapidly in response to *Atg7* deletion following tamoxifen induction (**Fig. 5D**) in the same time frame as the

This article is protected by copyright. All rights reserved.

elevation of SQSTM1/p62 and NQO1, the two known molecules upregulated in autophagy-deficient livers (6, 7). Furthermore, following tamoxifen treatment the inducible *Atg7*$^{\Delta Hep\text{-}ERT2}$ mice failed to upregulate FXR level in starvation (**Fig. 5E**). Taken together these results supported the regulatory role of autophagy in FXR expression under both fed and starved conditions.

Downregulation of FXR functionality is regulated by NRF2 in autophagy-deficient livers.

NRF2 can transcriptionally activate a number of genes including *Sqstm1* in autophagy deficient livers (6, 9-11). Deletion of *Nrf2* in autophagy-deficient livers reduced the accumulated SQSTM1 level (**Fig. 6A, Fig. S5A-B**). Conversely, NRF2 was important for the downregulation of FXR as co-deletion of *Nrf2* in autophagy deficient livers led to a significant restoration of FXR expression at both protein and mRNA (**Fig. 6A-B, Fig. S4B**) levels. Co-deletion of *Nrf2* was able to significantly reverse the expressional change of the major FXR targets, including *Shp, Bsep, Slc27a5/Bacs* (**Fig. 6C, Fig. S4C-D**) and *Ntcp* (**Fig. 3F**) in *Atg7* or *Atg5*-deficient livers. The downregulation of *Baat* was not reversed by Nrf2 deletion (**Fig. 6C**), suggesting that it might be subjected to additional regulation. We further showed that NRF2 activation alone pharmacologically or genetically could cause downregulation of FXR (**Fig. S6**). Such activations do not cause liver injury or autophagy deficiency (8).

FXR induces gene transcription by directly binding to FXRE (28, 30, 31). CHIP analysis effectively detected the binding of FXR to the FXRE sequence in the promoters of *Shp, Bsep* and *Ostβ* genes (**Fig. 6D**), but not in a coding region (**Fig. 6E**), in the normal livers. However, FXR binding to the target gene promoters was suppressed in autophagy-deficient

This article is protected by copyright. All rights reserved.

Accepted Article

livers, which could be significantly reversed by co-deletion of *Nrf2* (**Fig. 6D**). These data thus suggested that NRF2 negatively regulated FXR binding to its target gene promoters, possibly by reducing its expression level. Additionally, FXR binding to these sites was elevated in the livers deficient in *Nrf2* alone (**Fig. 6D**), suggesting that NRF2 could provide a counterbalance to FXR activity even at the basal level.

The discrepancy between reduced FXR binding to the FXRE of *Ostβ* (**Fig. 6D**) and an increased expression of this gene **(Fig. 3E**), and the ability of *Nrf2* co-deletion to reverse these changes suggested that *Nrf2* had an independent but more dominant control on *Ostβ* expression in the autophagy deficiency setting. Indeed, there is an *Nrf2*-binding ARE sequence in the *Ostβ* promoter (Khambu and Yin, unpublished observations).

Enhancement of FXR expression or activity alleviated cholestatic injury in autophagy-deficient livers

Because FXR can regulate the expression of genes involved in BA synthesis, secretion and reabsorption, downregulated FXR expression and activity in autophagy deficient livers could be an important contributing mechanism for the cholestasis in these livers.

To further examine this hypothesis, we treated 4-week old *Atg7*-deficient mice, which had about 40% of FXR expression (**Fig. 5C**), with a potent and selective nonsteroidal FXR agonist, GW4064 (33, 34) (**Fig. 7A**). FXR activity was stimulated based on the restored mRNA expression of its target genes, *Shp*, *Bsep*, *Slc27a5/Bacs*, and *Baat* (**Fig. 7B**). Re-expression of the BSEP molecules was also confirmed by immunoblotting and immunostaining (**Fig. 7C-D**), which showed a normal canalicular pattern. Note that SQSTM1 expression was not significantly changed at the protein or mRNA level by

This article is protected by copyright. All rights reserved.

Accepted Article

GW4064 treatment (**Fig. S5C-D**). Histological analysis of the liver in treated *Atg7*$^{\Delta Hep}$ mice revealed a significant reduction in the severity of ductular reaction and the number of CK19-positive ductular cells (**Fig7E**). Together with these changes, a significant reduction in blood bile acids and ALT levels, and improved liver/body weight ratio were observed (**Fig. 7F**), indicating that GW4064 was able to significantly correct cholestasis and liver injury caused by autophagy deficiency.

Alternatively, we administrated a constitutively activated *Fxr* construct, *Ad-VP16-Fxr* (17), at the time when the *Atg7* gene was deleted in the inducible *Atg7*$^{\Delta Hep\text{-}ERT2}$ mice (**Fig. 8A**). This treatment elevated the mRNA levels of *Fxr*, *Shp*, and *Bsep* in 10 days (**Fig. 8B**). The normalized BSEP expression was confirmed by immunoblotting (**Fig. 8C**) and immunostaining (**Fig. 8D**) assays in mice given *Ad-VP16-Fxr*. Similar to the treatment with GW4064, increased expression of FXR did not cause changes in SQSTM1 expression at the protein or mRNA level (**Fig. 8C, Fig. S5E-F**). The cholestasis was reversed as shown by the reversion of the elevated expression of *Mrp4* to the normal level (**Fig. 8B**), the reduced ductular reaction (**Fig. 8D**) and the normalization of blood BA level (**Fig. 8E**).

Taken together, autophagy deficiency in the liver led to the down-regulated expression of FXR and its target molecules, including BSEP, which could contribute to intracellular cholestasis. Enhancing FXR activities resorted BSEP expression, normalized blood BA level and ameliorated the injury phenotype. This study also indicated that an important function of normal autophagy is to maintain FXR functionality.

This article is protected by copyright. All rights reserved.

Accepted Article

Accepted Article

DISCUSSION

Autophagy regulates FXR expression and activity

A key finding of this study is the regulation of FXR expression and function by autophagy and the pathological consequence of the failure of such a regulation. We showed here that autophagy sustained FXR expression in fed condition and promoted FXR upregulation in starved condition. The expression of the target genes of FXR was affected correspondingly. Previous studies have shown that FXR can act as an inhibitory mechanism for autophagy in both fed and starved condition by regulating the transcriptional levels of several autophagy-related genes, such as *Lc3b* and *Atg7* (14, 15). Our data now show that autophagy and FXR can form a regulatory loop in which autophagy can maintain FXR functionality and FXR signaling can serve as a feedback suppression mechanism for autophagy (**Fig. 8F**). This dynamic relationship could provide an overall homeostasis of the two functions.

The reduced FXR functionality in autophagy-deficient livers could be resulted from several mechanisms. First, the transcriptional level of *Fxr* was reduced. Second, the ability of FXR to bind to FXRE in target genes was reduced, which would be in part due to the reduced level of FXR. Thirdly, the ratio of TMCA/TCA was increased in autophagy-deficient mice. Since TMCA is an antagonist of FXR (16) a higher TMCA/TCA ratio can lead to an enhanced antagonism against FXR activity as noted previously (16).

FXR expression decreased at both protein and mRNA levels, rapidly following the deletion of *Atg7* or *Atg5* no matter whether the deletion occurred at the embryonic or adult stage. NRF2 seems to mediate the mechanism, by which autophagy deficiency represses FXR functionality. NRF2 also affected the FXR binding to FXRE in the promoters of the

This article is protected by copyright. All rights reserved.

target genes. On the other hand, the mechanism by which activated autophagy promotes FXR expression following starvation or rapamycin treatment has yet to be defined. Interestingly, a previous study had shown that NRF2 could also activate FXR by a non-transcriptional mechanism via promoting its deacetylation in a cellular protection mode (35). It may be speculated that NRF2 might be involved in FXR regulation in both directions. But if that would be the case, the context, the mode of action and the way NRF2 is activated, would be all very different.

Being a major intracellular receptor of BA, FXR is activated by BA and in turn negatively regulates BA metabolism. FXR downregulation in autophagy-deficient condition could be a major contributing factor to the observed cholestasis phenotype. FXR normally upregulates BSEP to promote BA secretion (18, 36). We did not see the upregulation of BSEP in starved or rapamycin-treated livers where FXR was upregulated. But a significant suppression of BSEP expression was seen in autophagy-deficient condition. It seems that the influence of FXR on BSEP expression could be context-dependent and affected by other signals. Abnormal BSEP function is correlated with cholestasis (22, 23). FXR downregulation would likely be not the only factor causing cholestasis. However, augmentation of FXR functionality significantly restored BSEP expression, and reduced cholestasis and injury.

Since bile acid metabolism is closely coupled with cholesterol catabolism, autophagy may have a role in regulating cholesterol metabolism, which is evident from the elevated serum cholesterol level in autophagy-deficient mice (**Fig. 1E**, **Fig. S1E**). FXR is also broadly engaged in cholesterol, lipid and glucose metabolism in addition to bile acids metabolism (20, 30, 37, 38). Indeed, FXR upregulation under the condition of autophagy activation is most prominently associated with the upregulation of *Pepck* and *ApoE*, which are involved in

This article is protected by copyright. All rights reserved.

Accepted Article

metabolism of gluconeogenesis and lipids, respectively. It is thus conceivable that a normal autophagy function could have impacts on these processes via FXR. The functional significance of FXR upregulation and downregulation under different autophagy status may thus be distinct.

Autophagy regulates bile acids metabolism and autophagy-deficient liver injury is related to cholestasis.

Hepatic deficiency-induced liver injury is well documented (6-8) but the nature of the injury was not clear. Our findings indicate that cholestasis can be a major contributing factor to the liver injury based on the elevated bile acids level in the blood, the elevated hepatic bile acids level, the altered bile acid composition in the bile, the repressed expression of bile acids synthesis genes, the altered expression of both apical and basal-lateral transporters and the altered bile canalicular structure. These changes led us to determine FXR as a key mechanistic factor in the pathogenesis, and to identify the role of autophagy in the homeostasis of the FXR-bile acid metabolism.

Most of the metabolic functions of autophagy are known to be mediated by the recycling of nutrients or by the direct removal of unwanted organelles (2-4). However, the homeostatic role of autophagy in bile acids metabolism as shown in this study is mediated by a series of signaling events that are characterized by the alteration in FXR functionality. This demonstrates a new pattern of metabolism regulation by autophagy and suggests that the impact of autophagy on metabolism can be much broader than previously thought.

This article is protected by copyright. All rights reserved.

Accepted Article

Accepted Article

While the downregulation of BSEP can be a direct consequence of FXR downregulation, the cause of the altered expression of BA synthesis genes can be more convoluted. The four key synthesis genes (*Cyp7a1*, *Cyb8b1*, *Cyp27a1* and *Cyp7b1*) in the classical and alternative pathways were downregulated in the autophagy-deficient livers, likely in response to elevated hepatic BA levels. But the signaling leading to these changes have yet to be clearly depicted since the usual inhibitory signaling mediated by FXR might not work in the face of reduced FXR functionality in the autophagy-deficient livers. Expression of *Cyp7a1*, *Cyp8b1* and *Cyp27a1* in autophagy-deficient livers was restored with the co-deletion of *Nrf2*, which might simply reflect the fact that NRF2 corrected the cholestasis. Interestingly, *Cyp7b1* expression was not restored by co-deletion of *Nrf2*, suggesting that its expression has more complicated regulatory mechanisms in autophagy deficient livers.

One interesting but still yet to be fully investigated observation is that the ratio of taurine conjugated CA versus MCA is reversed in the autophagy-deficient livers. MCA is converted from chenodeoxycholic acid (CDCA), which is synthesized through both pathways (**Fig. S2A**). On the other hand, CA is synthesized only through the classical pathway, for which *Cyp8b1* is the key enzyme. In autophagy deficient livers *Cyp8b1* is significantly downregulated, thus favoring the generation of CDCA and MCA over CA, hence the higher ratio of TMCA/TCA. This looks similar to what is observed in *Cyp8b1*-deficient mice (19). The reversion in TMCA/TCA ratio can contribute to the inhibition of FXR function as discussed above.

It is noted that mice deficient in *Fxr* have key pathological features that are seen in the autophagy-deficient mice, including the significant downregulation of *Bsep*, abnormal expression of genes in bile acids synthesis, and elevated bile acids and cholesterol levels in

This article is protected by copyright. All rights reserved.

the blood (36). But *Fxr*-deficient mice had no significant liver injury, perhaps owing to that *Shp* expression is not entirely dependent on *Fxr* and can be compensated in the absence of *Fxr*. Consistently, mice deficient in both *Fxr* and *Shp* had severe liver injury (18), and both *Fxr* and *Shp* were downregulated in autophagy deficient livers (**Fig. 6C, Fig. S4C**). Additional mechanisms other than a simple reduction of *Fxr* can thus contribute to injury in autophagy-deficient livers (**Fig. 8F**).

NRF2 contributes to liver pathology by repression of FXR in autophagy deficient livers

Interestingly, co-deletion of *Nrf2* reversed most, if not all, of the liver pathologies associated with defective hepatic autophagy (6-8), indicating that NRF2 is the master determining factor for the pathology of the liver. However, the detrimental effect of NRF2 had been puzzling since NRF2 is generally involved in protective anti-oxidative stress response (9-12). The present study shows that a high level of NRF2 can contribute to the cholestatic injury of the liver, possibly by suppressing FXR functionality. In addition, NRF2 can cause HMGB1 release from autophagy-deficient hepatocytes, which contribute to the development of ductular reaction and tumor development in the livers (8). NRF2 can thus act on multiple pathways to exert its pathological effects.

Autophagy deficiency causes NRF2 to be highly activated due to displacement of KEAP1 by the accumulated p62/SQSTM1 proteins (6). NRF2 is best known for its ability to transcriptionally activate genes responsible for anti-oxidative stress (9-12) and genes involved in drug excretion (13), such as *Nqo1*, *Mrp3* and *Mrp4*. They are indeed elevated in autophagy deficient livers. *Sqstm1* is also upregulated by NRF2 (**Fig. 6A, Fig. S5**) as previously reported (6), but not by FXR in the autophagy deficient context, unlikely in other

This article is protected by copyright. All rights reserved.

Accepted Article

contexts (39). Most importantly, this study showed that activated NRF2 can cause transcriptional repression on genes such as *Fxr*. The repressive effect of NRF2 on gene transcriptions has not been well studied. The negative association with FXR expression provides a functionally relevant case for such investigations in future studies.

The reversion of the injury by FXR activation also suggests that FXR suppression by NRF2 is a key mechanism in which NRF2 mediates cholestatic liver injury associated with disturbed bile acids metabolism **(Fig.8F**). In addition, it should be noted that the detrimental effect of NRF2 needs to be distinguished from the reported protective effect of NRF2 in mice with normal autophagy function, but subjected to extra-hepatic cholestasis caused by bile duct ligation (40, 41). Thus the overall effect of NRF2 activation in liver pathobiology would be context dependent.

In summary, the present study has established a new regulatory pathway from autophagy to FXR via NRF2 and defined its significance in bile acids metabolism and in hepatic pathogenesis. This is a new model in which autophagy regulates metabolism independently of the recycling of macromolecules for direct nutritional use, but by affecting a series of signaling events. The autophagy-FXR regulatory loop may have important implications in metabolism broadly and in contexts other than autophagy deficiency or bile acids metabolism.

ACKNOWLEDGEMENTS

The authors would like to thank Dr. Bruno Stieger (University Hospital Zurich, Zurich, Switzerland) for the anti-BSEP and MRP2 antibodies, and Dr. Sabine Werner (Swiss Federal Institute of Technology, Zurich, Switzerland) for the Ca-Nrf2 liver samples. The CK19 and ZO-1 monoclonal antibodies were obtained from the Developmental Studies Hybridoma

This article is protected by copyright. All rights reserved.

Accepted Article

Bank, created by the NICHD, NIH, and maintained at Department of Biology, the University of Iowa, Iowa City, IA). We are grateful to Dr. Grace L Guo (Rutgers University, New Jersey, NJ) for advice on CHIP assay.

REFERENCES

1. Ohsumi Y. Historical landmarks of autophagy research. Cell Res 2014;24:9-23.
2. Czaja MJ, Ding WX, Donohue TM, Jr., Friedman SL, Kim JS, Komatsu M, Lemasters JJ, et al. Functions of autophagy in normal and diseased liver. Autophagy 2013;9:1131-1158.
3. Madrigal-Matute J, Cuervo AM. Regulation of Liver Metabolism by Autophagy. Gastroenterology 2016;150:328-339.
4. Boya P, Reggiori F, Codogno P. Emerging regulation and functions of autophagy. Nat Cell Biol 2013;15:713-720.
5. Mizushima N, Levine B, Cuervo AM, Klionsky DJ. Autophagy fights disease through cellular self-digestion. Nature 2008;451:1069-1075.
6. Komatsu M, Kurokawa H, Waguri S, Taguchi K, Kobayashi A, Ichimura Y, Sou YS, et al. The selective autophagy substrate p62 activates the stress responsive transcription factor Nrf2 through inactivation of Keap1. Nat Cell Biol 2010;12:213-223.
7. Ni HM, Woolbright BL, Williams J, Copple B, Cui W, Luyendyk JP, Jaeschke H, et al. Nrf2 promotes the development of fibrosis and tumorigenesis in mice with defective hepatic autophagy. J Hepatol 2014;61:617-625.
8. Khambu B, Huda N, Chen X, Antoine DJ, Li Y, Dai G, Kohler UA, et al. HMGB1 promotes ductular reaction and tumorigenesis in autophagy-deficient livers. J Clin Invest 2018;128:2419-2435.
9. Friling RS, Bensimon A, Tichauer Y, Daniel V. Xenobiotic-inducible expression of murine glutathione S-transferase Ya subunit gene is controlled by an electrophile-responsive element. Proc Natl Acad Sci U S A 1990;87:6258-6262.
10. Rushmore TH, Morton MR, Pickett CB. The antioxidant responsive element. Activation by oxidative stress and identification of the DNA consensus sequence required for functional activity. J Biol Chem 1991;266:11632-11639.
11. Ma Q. Role of nrf2 in oxidative stress and toxicity. Annu Rev Pharmacol Toxicol 2013;53:401-426.
12. Suzuki T, Yamamoto M. Molecular basis of the Keap1-Nrf2 system. Free Radic Biol Med 2015;88:93-100.
13. Maher JM, Dieter MZ, Aleksunes LM, Slitt AL, Guo G, Tanaka Y, Scheffer GL, et al. Oxidative and electrophilic stress induces multidrug resistance-associated protein transporters via the nuclear factor-E2-related factor-2 transcriptional pathway. Hepatology 2007;46:1597-1610.
14. Lee JM, Wagner M, Xiao R, Kim KH, Feng D, Lazar MA, Moore DD. Nutrient-sensing nuclear receptors coordinate autophagy. Nature 2014;516:112-115.
15. Seok S, Fu T, Choi SE, Li Y, Zhu R, Kumar S, Sun X, et al. Transcriptional regulation of autophagy by an FXR-CREB axis. Nature 2014;516:108-111.
16. Sayin SI, Wahlstrom A, Felin J, Jantti S, Marschall HU, Bamberg K, Angelin B, et al. Gut microbiota regulates bile acid metabolism by reducing the levels of tauro-beta-muricholic acid, a naturally occurring FXR antagonist. Cell Metab 2013;17:225-235.

This article is protected by copyright. All rights reserved.

Accepted Article

17. Li S, Hsu DD, Li B, Luo X, Alderson N, Qiao L, Ma L, et al. Cytoplasmic tyrosine phosphatase Shp2 coordinates hepatic regulation of bile acid and FGF15/19 signaling to repress bile acid synthesis. Cell Metab 2014;20:320-332.
18. Anakk S, Watanabe M, Ochsner SA, McKenna NJ, Finegold MJ, Moore DD. Combined deletion of Fxr and Shp in mice induces Cyp17a1 and results in juvenile onset cholestasis. J Clin Invest 2011;121:86-95.
19. Li-Hawkins J, Gafvels M, Olin M, Lund EG, Andersson U, Schuster G, Bjorkhem I, et al. Cholic acid mediates negative feedback regulation of bile acid synthesis in mice. J Clin Invest 2002;110:1191-1200.
20. Li T, Chiang JY. Bile acid signaling in metabolic disease and drug therapy. Pharmacol Rev 2014;66:948-983.
21. Gerloff T, Stieger B, Hagenbuch B, Madon J, Landmann L, Roth J, Hofmann AF, et al. The sister of P-glycoprotein represents the canalicular bile salt export pump of mammalian liver. J Biol Chem 1998;273:10046-10050.
22. Wang R, Salem M, Yousef IM, Tuchweber B, Lam P, Childs SJ, Helgason CD, et al. Targeted inactivation of sister of P-glycoprotein gene (spgp) in mice results in nonprogressive but persistent intrahepatic cholestasis. Proc Natl Acad Sci U S A 2001;98:2011-2016.
23. Wang L, Soroka CJ, Boyer JL. The role of bile salt export pump mutations in progressive familial intrahepatic cholestasis type II. J Clin Invest 2002;110:965-972.
24. Johnson DR, Habeebu SS, Klaassen CD. Increase in bile flow and biliary excretion of glutathione-derived sulfhydryls in rats by drug-metabolizing enzyme inducers is mediated by multidrug resistance protein 2. Toxicol Sci 2002;66:16-26.
25. Oude Elferink RP, Ottenhoff R, van Wijland M, Smit JJ, Schinkel AH, Groen AK. Regulation of biliary lipid secretion by mdr2 P-glycoprotein in the mouse. J Clin Invest 1995;95:31-38.
26. Berge KE, Tian H, Graf GA, Yu L, Grishin NV, Schultz J, Kwiterovich P, et al. Accumulation of dietary cholesterol in sitosterolemia caused by mutations in adjacent ABC transporters. Science 2000;290:1771-1775.
27. Yeh TH, Krauland L, Singh V, Zou B, Devaraj P, Stolz DB, Franks J, et al. Liver-specific beta-catenin knockout mice have bile canalicular abnormalities, bile secretory defect, and intrahepatic cholestasis. Hepatology 2010;52:1410-1419.
28. Laffitte BA, Kast HR, Nguyen CM, Zavacki AM, Moore DD, Edwards PA. Identification of the DNA binding specificity and potential target genes for the farnesoid X-activated receptor. J Biol Chem 2000;275:10638-10647.
29. Pircher PC, Kitto JL, Petrowski ML, Tangirala RK, Bischoff ED, Schulman IG, Westin SK. Farnesoid X receptor regulates bile acid-amino acid conjugation. J Biol Chem 2003;278:27703-27711.
30. Wang YD, Chen WD, Moore DD, Huang W. FXR: a metabolic regulator and cell protector. Cell Res 2008;18:1087-1095.
31. Thomas AM, Hart SN, Kong B, Fang J, Zhong XB, Guo GL. Genome-wide tissue-specific farnesoid X receptor binding in mouse liver and intestine. Hepatology 2010;51:1410-1419.
32. Song X, Chen Y, Valanejad L, Kaimal R, Yan B, Stoner M, Deng R. Mechanistic insights into isoform-dependent and species-specific regulation of bile salt export pump by farnesoid X receptor. J Lipid Res 2013;54:3030-3044.
33. Maloney PR, Parks DJ, Haffner CD, Fivush AM, Chandra G, Plunket KD, Creech KL, et al. Identification of a chemical tool for the orphan nuclear receptor FXR. J Med Chem 2000;43:2971-2974.

This article is protected by copyright. All rights reserved.

Accepted Article

34. Liu Y, Binz J, Numerick MJ, Dennis S, Luo G, Desai B, MacKenzie KI, et al. Hepatoprotection by the farnesoid X receptor agonist GW4064 in rat models of intra- and extrahepatic cholestasis. J Clin Invest 2003;112:1678-1687.
35. Kay HY, Kim WD, Hwang SJ, Choi HS, Gilroy RK, Wan YJ, Kim SG. Nrf2 inhibits LXRalpha-dependent hepatic lipogenesis by competing with FXR for acetylase binding. Antioxid Redox Signal 2011;15:2135-2146.
36. Sinal CJ, Tohkin M, Miyata M, Ward JM, Lambert G, Gonzalez FJ. Targeted disruption of the nuclear receptor FXR/BAR impairs bile acid and lipid homeostasis. Cell 2000;102:731-744.
37. Fiorucci S, Mencarelli A, Palladino G, Cipriani S. Bile-acid-activated receptors: targeting TGR5 and farnesoid-X-receptor in lipid and glucose disorders. Trends Pharmacol Sci 2009;30:570-580.
38. Zhu Y, Li F, Guo GL. Tissue-specific function of farnesoid X receptor in liver and intestine. Pharmacol Res 2011;63:259-265.
39. Haga S, Yimin, Ozaki M. Relevance of FXR-p62/SQSTM1 pathway for survival and protection of mouse hepatocytes and liver, especially with steatosis. BMC Gastroenterol 2017;17:9.
40. Okada K, Shoda J, Taguchi K, Maher JM, Ishizaki K, Inoue Y, Ohtsuki M, et al. Nrf2 counteracts cholestatic liver injury via stimulation of hepatic defense systems. Biochem Biophys Res Commun 2009;389:431-436.
41. Weerachayaphorn J, Mennone A, Soroka CJ, Harry K, Hagey LR, Kensler TW, Boyer JL. Nuclear factor-E2-related factor 2 is a major determinant of bile acid homeostasis in the liver and intestine. Am J Physiol Gastrointest Liver Physiol 2012;302:G925-936.

Accepted Article

This article is protected by copyright. All rights reserved.

Accepted Article

FIGURE LEGENDS

Figure 1. Autophagy deficiency causes cholestasis.

(**A-C**). Sera from mice of different genotypes were analyzed for the level of indicated parameters (n=3-7/group). (**D**) Kinetic analysis of blood chemistry in $Atg7^{Hep\text{-}ERT2}$ mice from D0 to D30 after induction of *Atg7* deletion by tamoxifen (n=3/group). (**E**) The amount of bile acids was determined in the liver, in the bile-containing gallbladder, and in the intestine of the *Atg7*-floxed and -deleted mice (n=8-12/group). (**F**) The bile acids pool (gall bladder + liver + intestine), and the pool normalized with the body weight (n=8-11/group). *Atg7 F/F*: *Atg7*-floxed control mice, *Atg7-/-*: hepatic *Atg7*-deficient mice, *Nrf2-/-*: *Nrf2*-deficient mice, *Atg7/Nrf2-/-*: *Nrf2*-deficient and hepatic *Atg7*-deficient mice. *: $p<0.05$; ***: $p<0.001$; n.s.: no significance.

Figure 2. Autophagy deficiency leads to disturbance in bile acids metabolism.

(**A-C**).The hepatic mRNA levels of indicated genes were quantified in 9-week old mice of different genotypes. (**D-E**) The compositions of taurine-conjugated (D) and unconjugated (E) bile acids in the bile were analyzed. *: $p<0.05$; **: $p<0.01$; ***: $p<0.001$; n. s.: no significance; n = 3 (A-C), or 4/group (D-E).

Figure 3. Autophagy deficiency alters the expression of hepatocyte transporters.

(**A-B**). Livers of 9 week-old mice of different genotypes were examined for BSEP by immunoblotting assay, which was quantified by densitometry. (**C**). Liver sections from mice of different genotypes were immunostained with anti-BSEP. Framed areas are enlarged and shown in separate panels (a-d). Arrowheads and arrows represent different morphology of bile canalicular conduits between neighboring hepatocytes. (**D**). The mRNA levels of indicated apical transporters were determined. (**E**).The mRNA levels of the indicated basolateral systemic transporters were determined. (**F**).The mRNA levels of the indicated

This article is protected by copyright. All rights reserved.

basolateral enterohepatic transporters were determined. *Atg5 F/F*: *Atg5*-floxed control mice, *Atg5-/-*: hepatic *Atg5*-deficient mice. *: p<0.05; **: p<0.01; ***: p<0.001. n=3-5/group.

Figure 4. Autophagy deficiency causes abnormality in bile canaliculi.

(**A**). Liver sections from mice of different genotypes were immunostained with anti-MRP2. Framed areas are enlarged and shown in separate panels (a-d). Arrows indicate enhanced signals of MRP2 in *Atg7*-deficient livers. (**B**). Electron microscopic examination of the bile canaliculi in livers of different genotypes. Two or three examples of the bile canaliculi in each genotype were shown. Panels a1-a2 show normal canaliculi in the floxed *Atg7* liver. The example in panel a1 was enlarged in panel a1'. Panel b1-b3 show enlarged and swollen bile canaliculi in *Atg7*-deficient liver, with the loss of microvilli and deposition of amorphous membranous materials. Panels c1-c3 show largely normal bile canaliculi in *Atg7/Nrf2*-doubly deficient liver. White arrow indicates the tight junction between the adherent hepatocytes. BC: bile canaliculus. (**C**). Livers from mice of different genotypes were sectioned and immunostained with an anti-ZO-1. The framed areas were enlarged and displayed in subpanels (a-e). Arrows indicated distorted ZO-1 staining pattern in *Atg7*-deficient livers. (**D**). Immunostaining with anti-β-CATENIN in *Atg7*-floxed and *Atg7*-deficient livers. (**E**). Livers sections were stained with rhodamine-phalloidin. n =3/group.

Figure 5. Autophagy regulates hepatic FXR expression.

(**A-B**). Mice were given rapamycin (4 mg/kg, i.p. Rap) or subjected to starvation (Stv) for 24 hours. The hepatic protein level (A), or mRNA levels of *Fxr* and its targets (B) was determined. Densitometry of the protein was conducted (A). (**C**). Liver lysates from mice of given genotypes and ages (week) were examined by immunoblotting assay, and the relative expression levels were quantified by densitometry. (**D**). $Atg7^{\Delta Hep\text{-}ERT2}$ mice were given 4-OHT on Day 1 and Day 2 to induce hepatic deletion of *Atg7*. Group D0 were mice receiving vehicle control. The livers were removed at different times (Day 5 to Day 20) and analyzed

This article is protected by copyright. All rights reserved.

Accepted Article

by immunoblotting assay. The densitometric levels of proteins shown in panel E were normalized to that of GAPDH, and to the Day 0 control group. The liver/body ratio relative to that of Day 0, which is defined as 100%. (**E**). *Atg7*$^{\Delta Hep\text{-}ERT2}$ mice were given 4-OHT or vehicle as in panel E. Mice were subjected to starvation (Stv) on Day 6 and analyzed 24 hours later (Group D7). Densitometry for the level of FXR was conducted. *: $p<0.05$; **: $p<0.01$; n.s.: no significance; n =3-5 mice/group.

Figure 6. NRF2 is requried for FXR downreguation in autophagy deficient livers.

(**A-B**). The hepatic protein (A) or mRNA (B) levels of FXR/*Fxr* were quantified in 9-week old mice of different genotypes with or without *Atg7* deficiency. The protein level of FXR was quantified by densitometry. (**C**) The hepatic mRNA levels of *Fxr* targets were determined in mice of different genotypes. (**D-E**) Hepatic lysates from mice of different genotypes were subjected to CHIP analysis using an anti-FXR antibody or a control IgG. Quantitative PCR was performed using primers for the FXR-binding region in the promotors of *Shp, Bsep* or *Ostβ* (D), or primers for a coding region of *Shp* (E) as the control. Data shown are average of three independent experiments. * $P<0.05$, ** $P<0.01$, *** $P<0.00$, n.s.: no significance; n=3 (D-E) or 4 (B-C)/group.

Figure 7. Stimulation of FXR reduces cholestatic liver injury.

(**A**) The schedule for the treatment of *Atg7*-deficient mice with a FXR agonist, GW4064 (30 mg/kg, i.p). Control mice were given vehicle control (corn oil). Mice were analyzed 2 days after the last injection. (**B**) Hepatic mRNA levels of indicated genes were analyzed. (**C**) Liver lysates were analyzed by immunoblotting for BSEP, which was quantified by densitometry. (**D**). Liver sections were immunostaining for BSEP. Arrows indicate the typical cannalicular expression pattern of BSEP. (**E**) Livers sections were subjected to the indicated staining (scale at x200 or as indicated). Arrows indicate clusters of ductular cells, which was reduced in treated group. (**F**). *Atg7*-floxed and -deleted mice treated with or

This article is protected by copyright. All rights reserved.

Accepted Article

without GW4064 were analyzed for total blood bile acids, ALT levels and the liver/body weight ratio. *: p<0.05; **: p<0.01; ***: p<0.001; n=6 mice/group.

Figure 8. Restoration of FXR expression reduces cholestasis in autphagy-deficient livers.

(**A**). Schematic diagram showing the treatment of *Atg7*$^{Hep\text{-}ERT2}$ mice with 4-OHT and adenovirus carrying *VP16* or *VP16-Fxr*. (**B**). The mRNA levels of indicated genes were analyzed by qRT-PCR in liver samples from *Atg7*$^{Hep\text{-}ERT2}$mice receiving the designated treatment. (**C**). Liver lysates were from *Atg7*$^{Hep\text{-}ERT2}$ mice receiving the designated treatment were analyzed by immunoblotting assay. (**D**). Livers from *Atg7*$^{Hep\text{-}ERT2}$ mice receiving the designated treatment were stained with an anti-BSEP antibody (upper row) or Hematoxylin-Eosin (lower row). Arrows indicated the typical cannalicular pattern of BSEP distribution. (**E**). Serum total bile acid levels were determined. (**F**). A model for the role of FXR in the liver injury caused by autophagy deficiency. Autophagy sustains FXR function whereas FXR suppresses autophagy at both fed and starved conditions, where FXR can be viewed as a feedback suppression mechanism for autophagy. Downregulation of FXR during autophagy deficiency can lead to cholestasis, contributing to the liver injury. NRF2 activation in autophagy deficiency can further enhance SQSTM1 expression and may cause additional insults to the liver. *: p<0.05; **: p<0.01; ***: p<0.001; n = 4-5/group.

This article is protected by copyright. All rights reserved.

Accepted Article

Figure 1

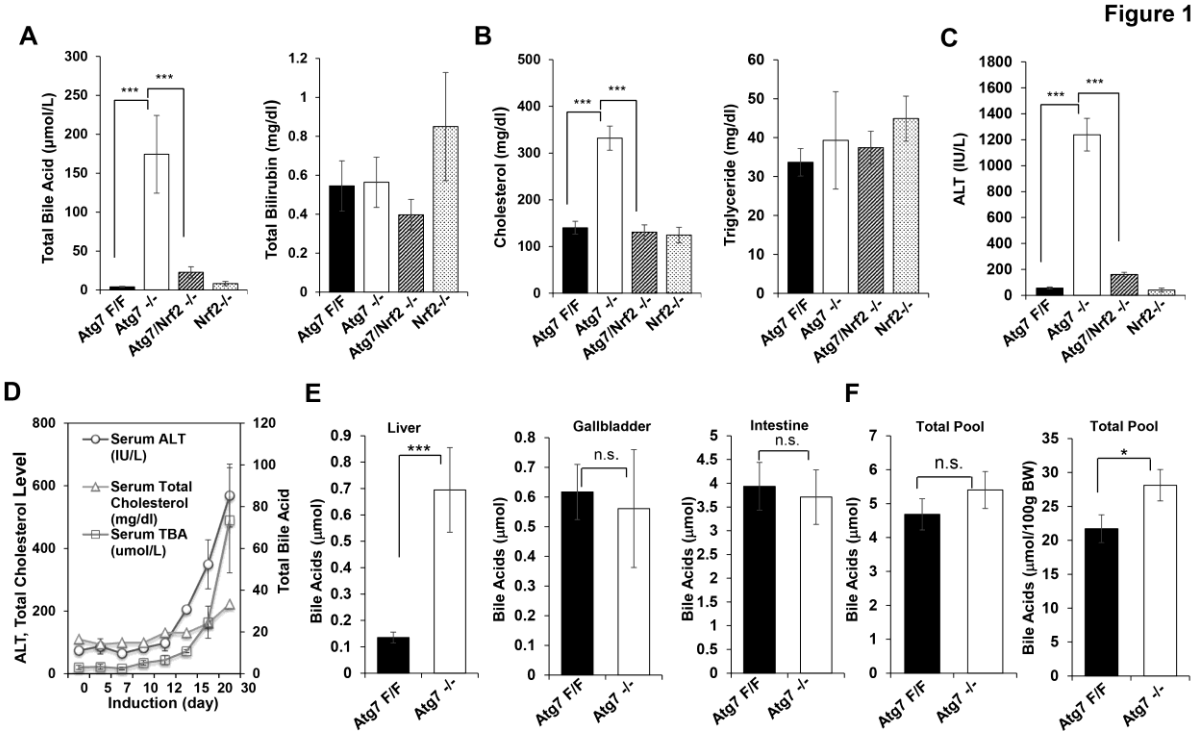

This article is protected by copyright. All rights reserved.

Accepted Article

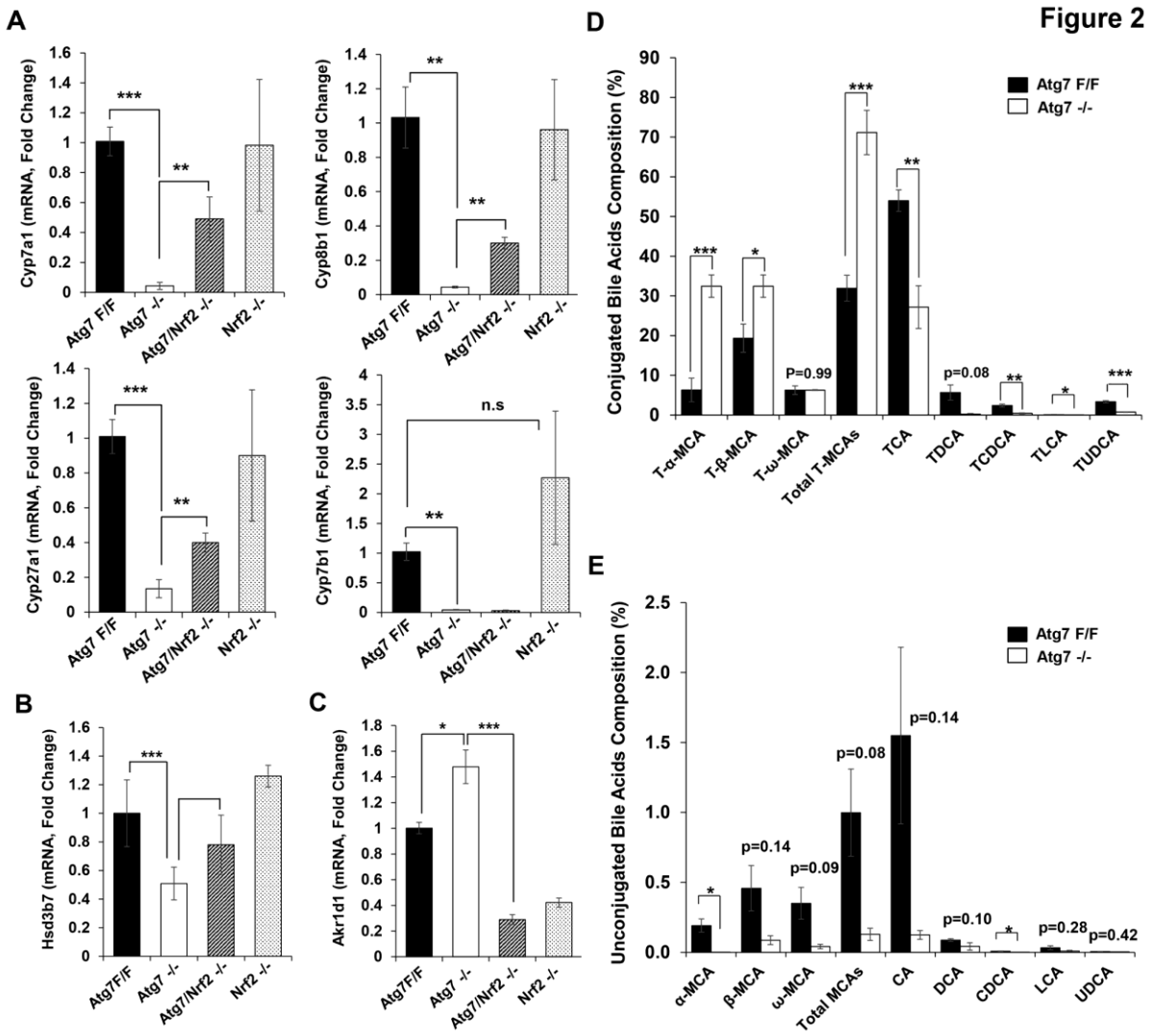

This article is protected by copyright. All rights reserved.

Accepted Article

Figure 3

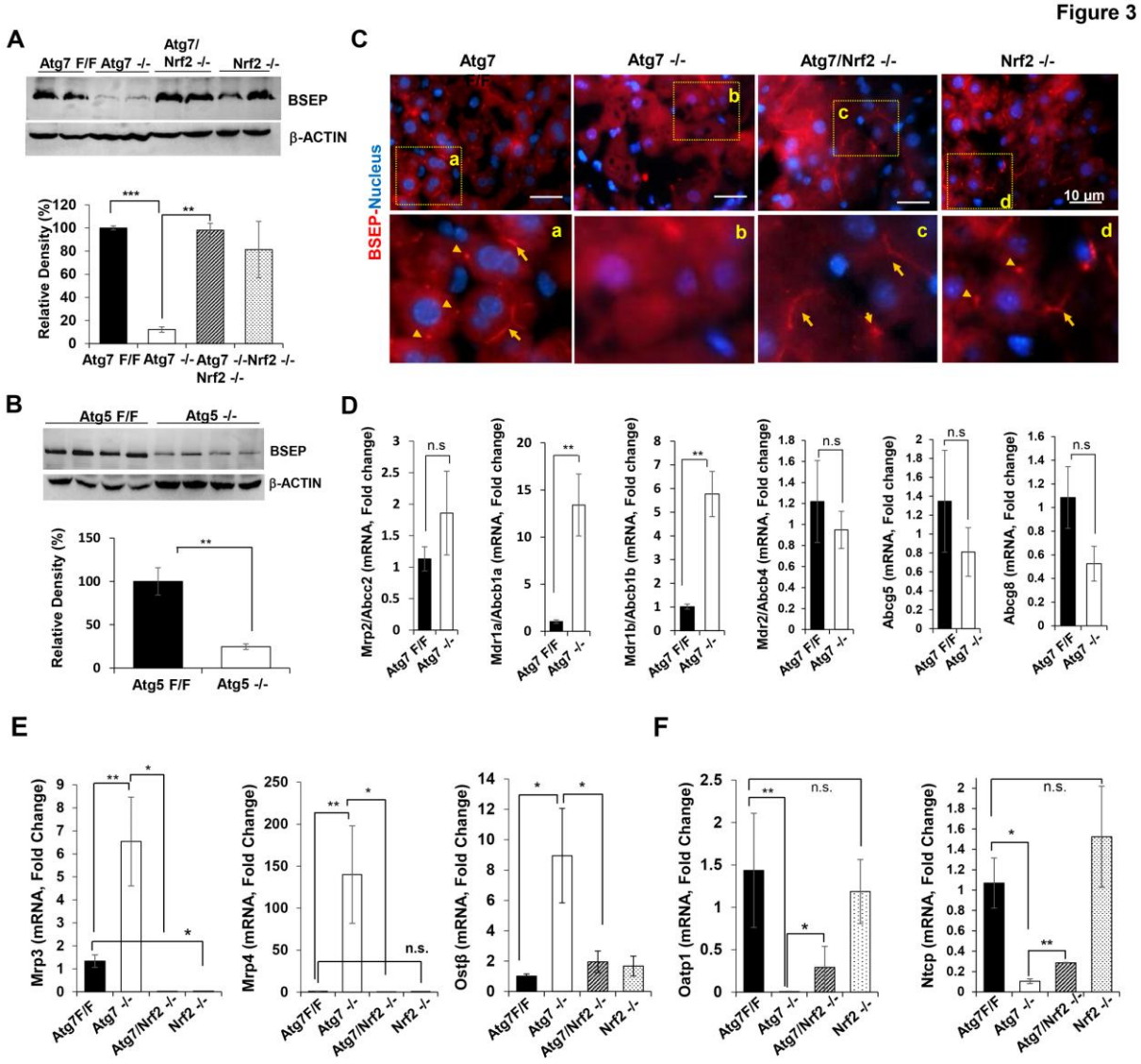

This article is protected by copyright. All rights reserved.

Accepted Article

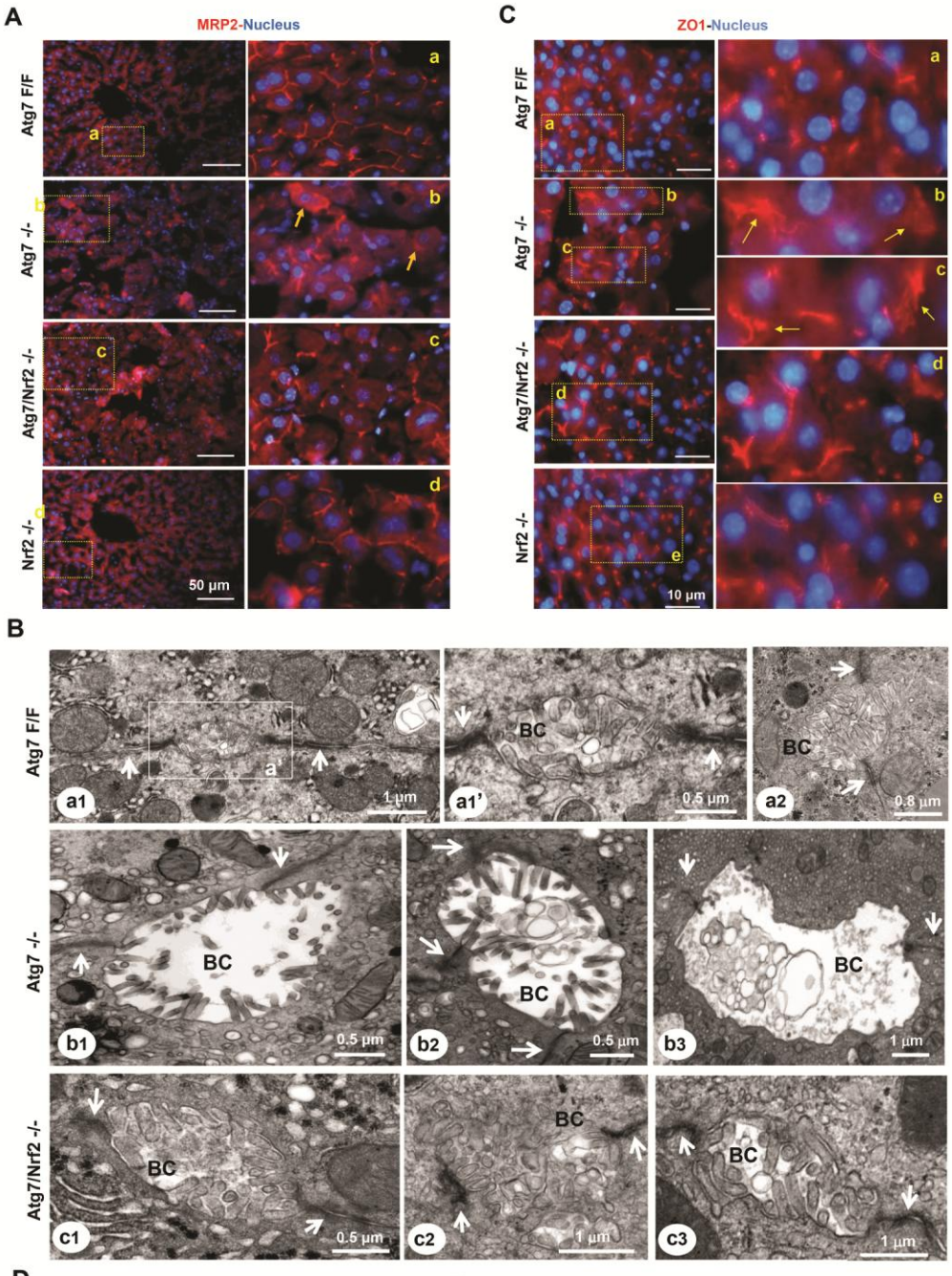

This article is protected by copyright. All rights reserved.

Accepted Article

Figure 5

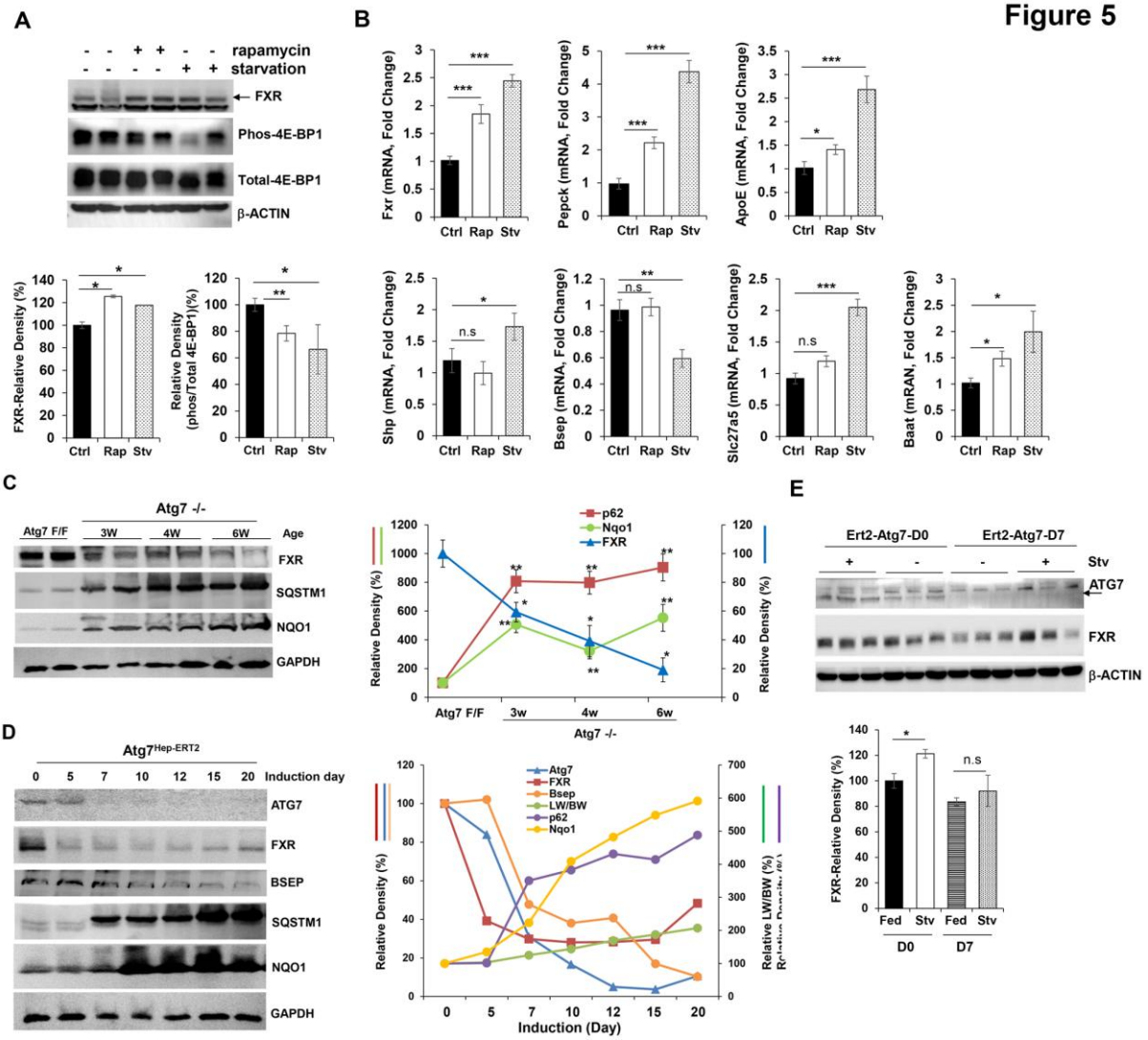

This article is protected by copyright. All rights reserved.

Accepted Article

Figure 6

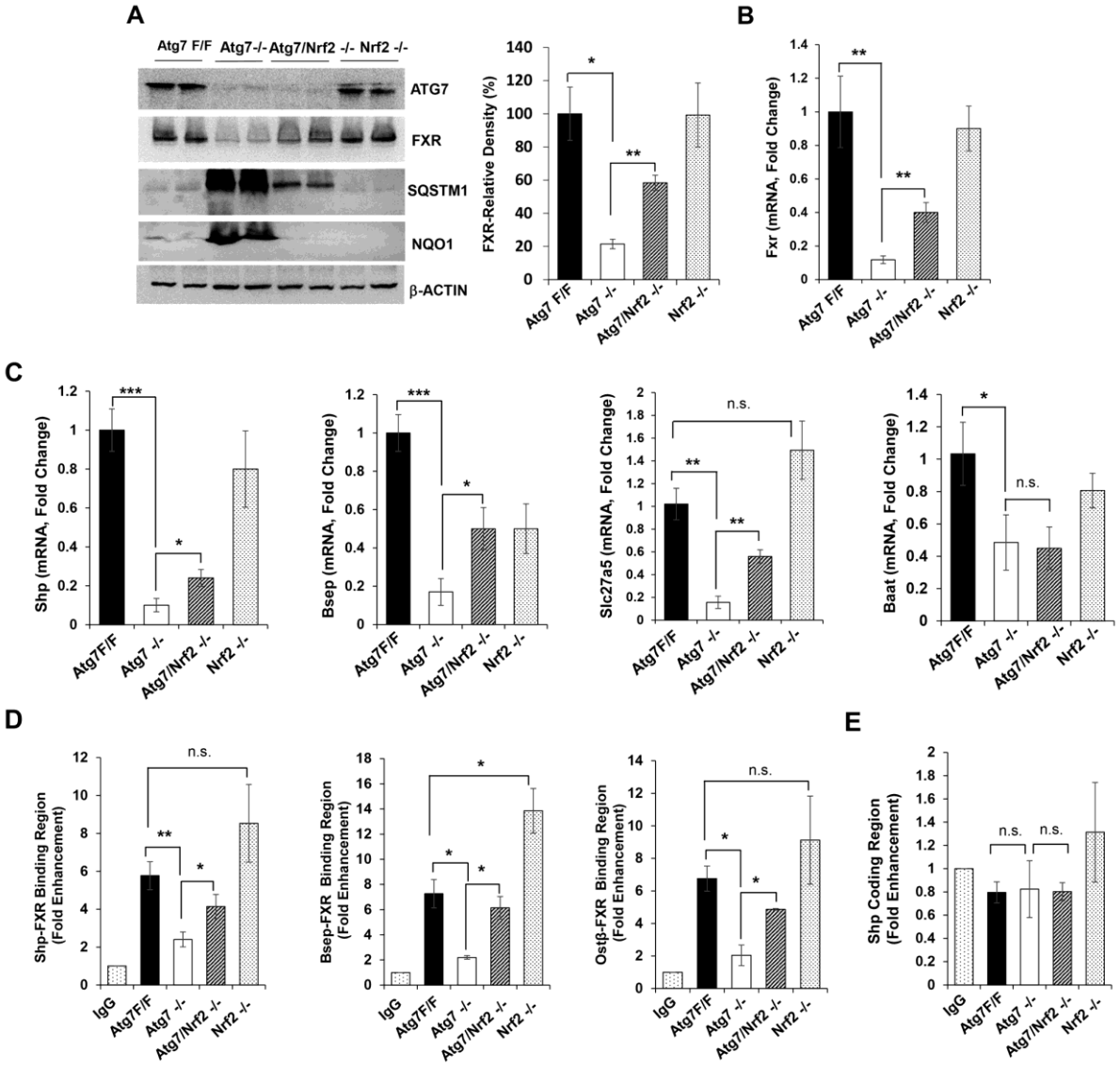

This article is protected by copyright. All rights reserved.

Accepted Article

Figure 7

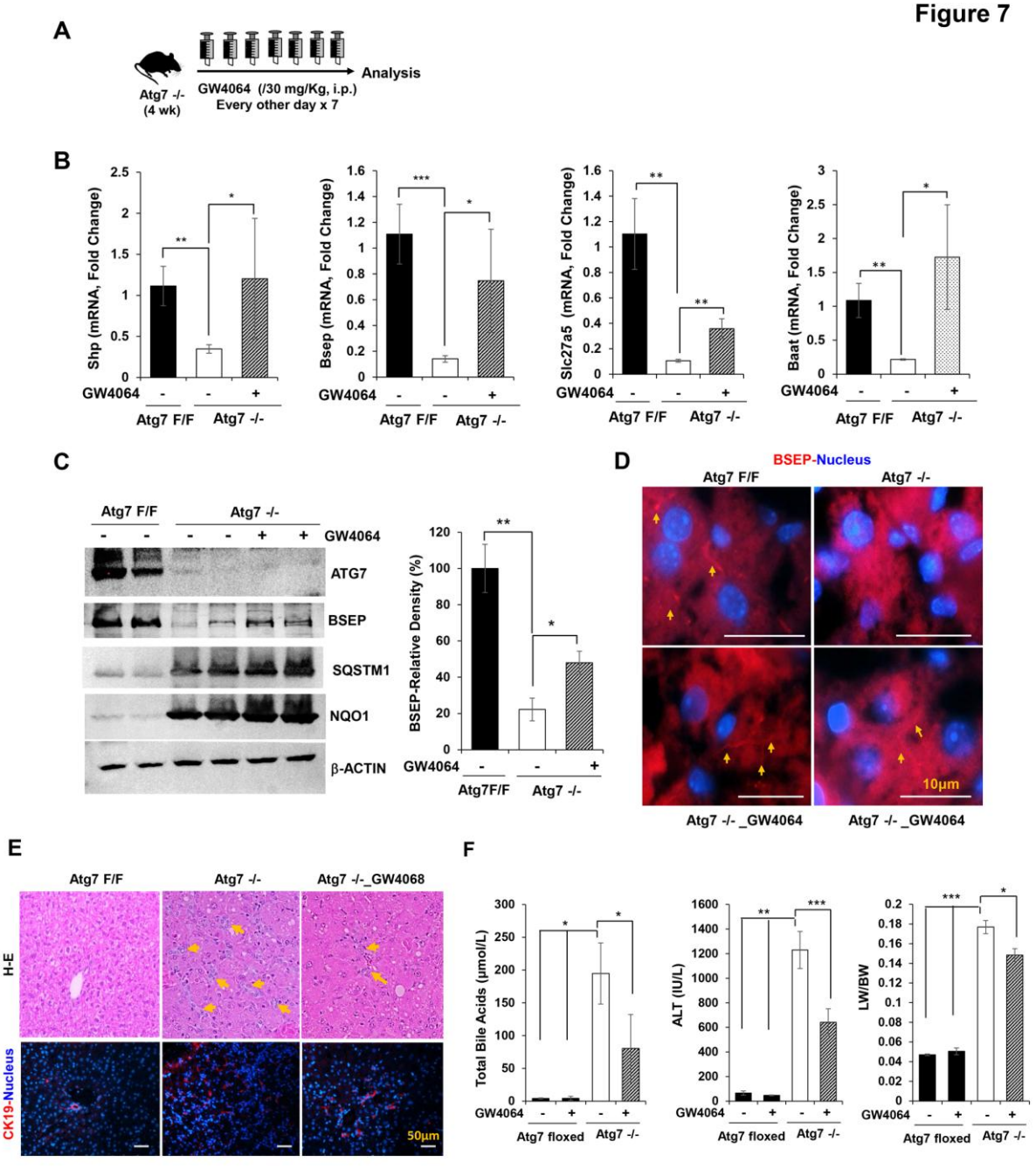

This article is protected by copyright. All rights reserved.

Accepted Article

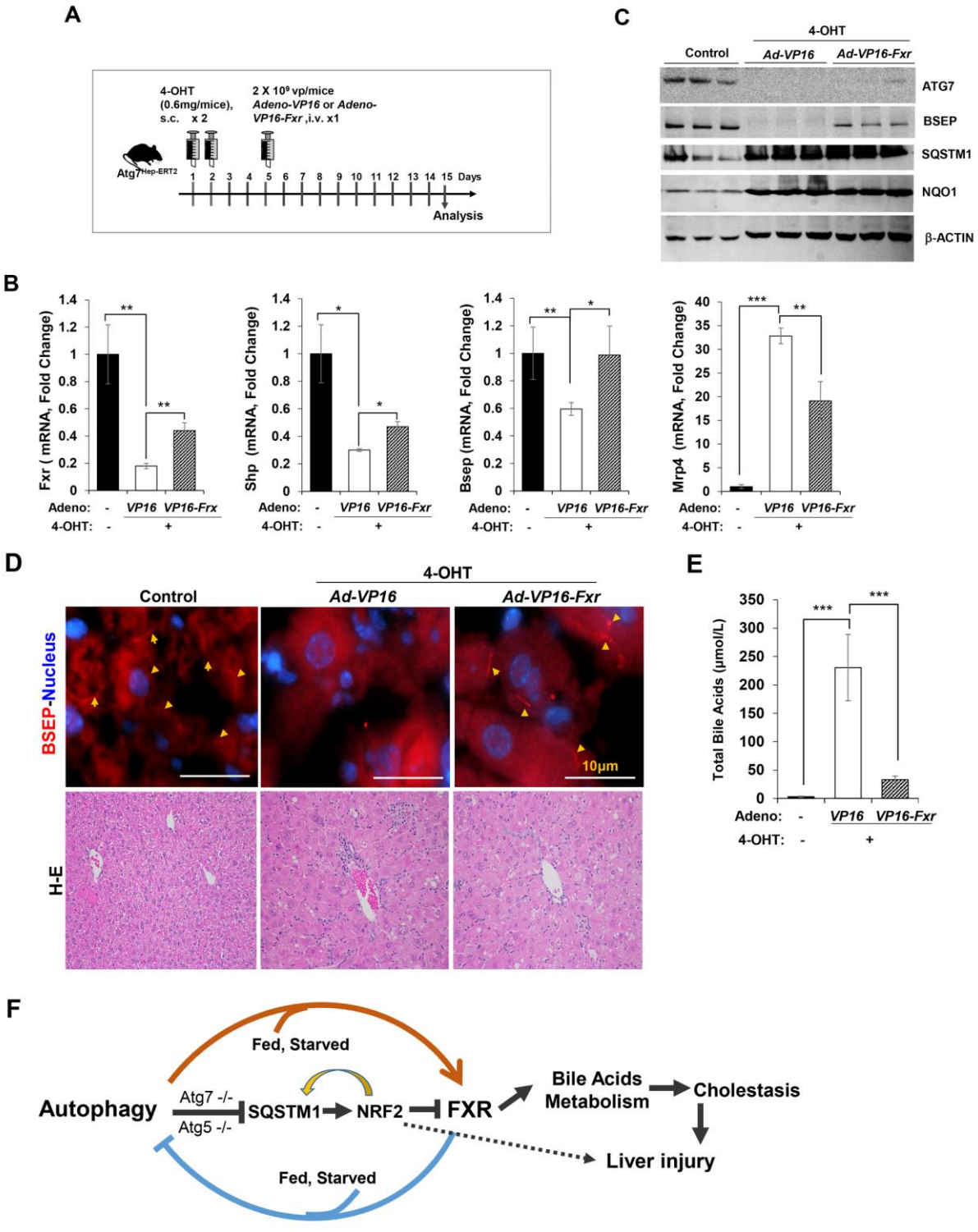

This article is protected by copyright. All rights reserved.